DOI: 10.1002/chem.200500893

Near Monodisperse TiO_2 Nanoparticles and Nanorods

Xiao-Lin Li, Qing Peng, Jia-Xiang Yi, Xun Wang, and Yadong Li*[a]

Abstract: Highly crystalline, near monodisperse TiO_2 nanoparticles, nanorods and their metal-ion-doped (Sn^{4+}, Fe^{3+}, Co^{2+}, and Ni^{2+}, etc.) derivatives have been prepared by well-controlled solvothermal reactions. Through adjusting the reaction parameters, such as reaction temperature, duration, and concentration of the reactants, the size, shape, and dispersibility of the products can be controlled. A possible reaction mechanism can be proposed based on experimental evidence.

Keywords: nanoparticles · nanorods · nanostructures · titanium

Introduction

Metal oxides produced from solution-phase synthetic routes have a strong tendency to form thin ceramic films at high temperatures, which is one of the most important forms of metal oxide in industrial applications. Therefore, scientists are devoting continuous effort to design novel solution-phase reactions to prepare these functional metal oxides.[1–5] Among them, the hydrolysis of metal alkoxide is especially popular.[1–3] However, alkoxide precursors are often too reactive, forming large complex molecules upon exposure in ambient humidity. Hence, modifying the ligands around the metal ions and controlling their modes of hydrolysis are extremely important to tailor hydrolysis and condensation rates, to yield high-quality metal oxides. Metal alkoxides modified by carboxylic acid and nonhydrolytic sol–gel routes have been applied to the synthesis of metal oxides recently.[6–7] In spite of these efforts, it is still not possible to synthesize thin films of high quality (high crystallization, controlled size, and good dispersibility in solvents) metal oxides. In this manuscript, using TiO_2 as an example, we have systematically demonstrated a solvothermal method to prepare highly crystalline, near monodisperse, and organic-solvent-dispersible metal oxides by controlling the conditions of the hydrolysis reaction.

[a] Dr. X.-L. Li, Dr. Q. Peng, J.-X. Yi, Dr. X. Wang, Prof. Y. Li
Department of Chemistry, Tsinghua University
Beijing, 100084 (P. R. China)
Fax: (+86) 10-6278-8765
E-mail: ydli@tsinghua.edu.cn

Supporting information for this article is available on the WWW under http://www.chemeurj.org/ or from the author.

TiO_2 is an important, wide-bandgap semiconductor and has been intensively studied because of its outstanding chemicophysical properties and unique applications in batteries, photocatalysis, water splitting, degradation of organic contaminants, photoinduced hydrophilicity, and photoelectrochromic windows, etc.[8–16] Depending on the applications, the TiO_2 components must fulfill a wide variety of requirements in terms of particle size, size distribution, morphology, crystallinity, and phase. Up to now, many TiO_2 nanostructures, including hollow spheres, nanotubes, nanowires, and mesoporous structures[8,9,17–28] have been synthesized. It has been found that highly crystalline, organic-solvent-dispersible TiO_2 with good surface properties (hydroxylation, defects, and surface area, etc.) and controlled sizes display well-tailored chemicophysical characteristics and the ability to form large-area films. Thus they are expected to greatly improve the technological performance of TiO_2 in many applications, such as solar cells, photocatalysis, and so forth. There have been several research groups (Colvin's, Alivisatos's, Weller's, Niederberger's, Wang's, etc.) that have reported nonaqueous, solution-based methods to prepare this kind of TiO_2 nanocrystallines.[22–26] Here, we developed a solvothermal method; by controlling the hydrolyzation reaction of $Ti(OBu)_4$ (Bu refers to $-C_4H_9$) using NH_4HCO_3 and linoleic acid (LA), redispersible TiO_2 nanorods and nanoparticles were successfully synthesized.[27] In this manuscript, we fully demonstrate the reaction mechanism and formation process of these highly crystalline, near monodisperse and re-dispersible TiO_2 nanoparticles and nanorods by controlling the solvothermal reaction parameters, like reaction temperatures, concentrations, reaction durations, and so forth. Also we report the solvothermal synthesis of metal-ion-doped (Sn^{4+}, Fe^{3+}, Co^{2+} and Ni^{2+}, etc) derivatives of TiO_2. This strategy provides an effective method for the synthesis

of high-quality, re-dispersible TiO_2 nanocrystallines and offers better opportunity for further investigation of their properties and applications. Furthermore, the procedure used may be developed into a general method for the synthesis of other metal-doped TiO_2 or other metal-oxide nanocrystalline materials. Recently, using an improved approach, our group has demonstrated a general method to obtain various kinds of crystalline, near-monodisperse nanoparticles.[28]

Results and Discussion

Typical X-ray diffraction (XRD) patterns of as-synthesized TiO_2 nanoparticles and nanorods were taken on a Bruker D8-advance X-ray powder diffractometer with $Cu_{K\alpha}$ radiation ($\lambda = 1.54178$ Å). As shown in Figure 1, the reflection peaks have been assigned to pure anatase phase TiO_2 with lattice constants of $a = 3.785$ Å and $c = 9.514$ Å, (JCPDS card No: 21–1272).

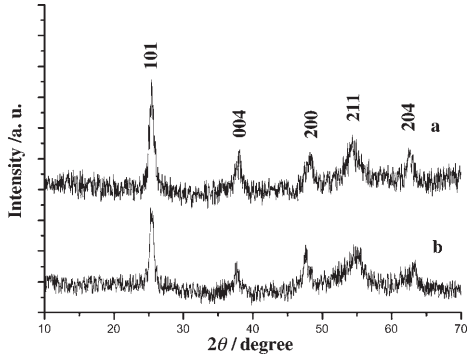

Figure 1. Typical XRD pattern of a) TiO_2 nanoparticles and b) TiO_2 nanorods.

The size and morphology of the as-synthesized TiO_2 nanoparticles were characterized by transition electron microscopy (TEM, Hitachi Model H-800). Figures 2 and b show the different magnification TEM images of TiO_2 nanoparticles. The nanoparticles were well spaced on the grid, because the surfaces of the particles were capped by LA. Based on the TEM characterization, as-synthesized TiO_2 nanoparticles are almost all in a spherelike morphology with a nearly monodisperse diameter of about 12 nm. High-resolution TEM (HRTEM, JEOL-2010F) provided further insight into the structure and crystallinity of the products (Figure 2c). The inset HRTEM image of a spherical nanoparticle in Figure 2c shows a well-crystallized structure with lattice fringes of about 0.35 nm, corresponding to the (101) planes of anatase TiO_2. Figure 2d shows a typical selected-area electron diffraction (SAED) pattern, in which all the reflections have been indexed. The composition of the nanoparticles was characterized by energy-dispersive X-ray spectroscopy (EDX); the results showed that the molar ratio of Ti and O in the sample is around 1:2 (the spectrum is not shown).

Typical TEM images of TiO_2 nanorods are provided in Figure 3. Figure 3a illustrates a large amount of TiO_2 nano-

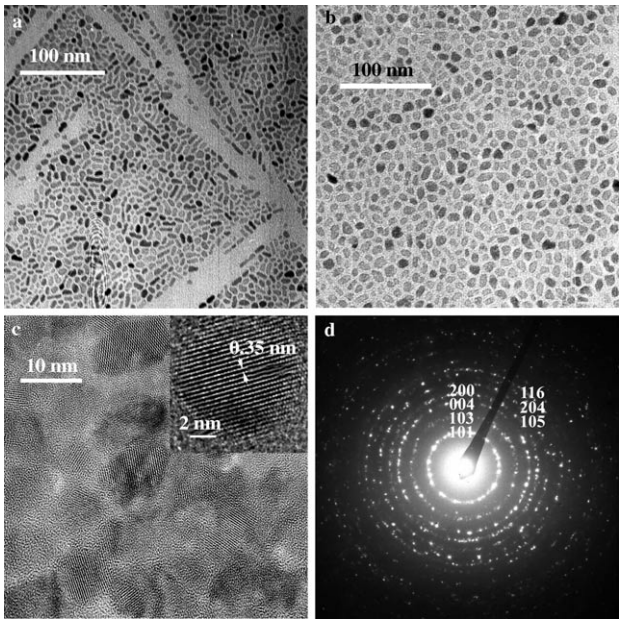

Figure 2. TEM images of TiO_2 nanoparticles: a,b) TEM images at different magnification, c) HRTEM image of TiO_2 nanoparticles (inset is an enlarged HRTEM image of an individual spherical particle; the lattice fringes are about 0.35 nm), and d) SAED pattern of TiO_2 nanoparticles.

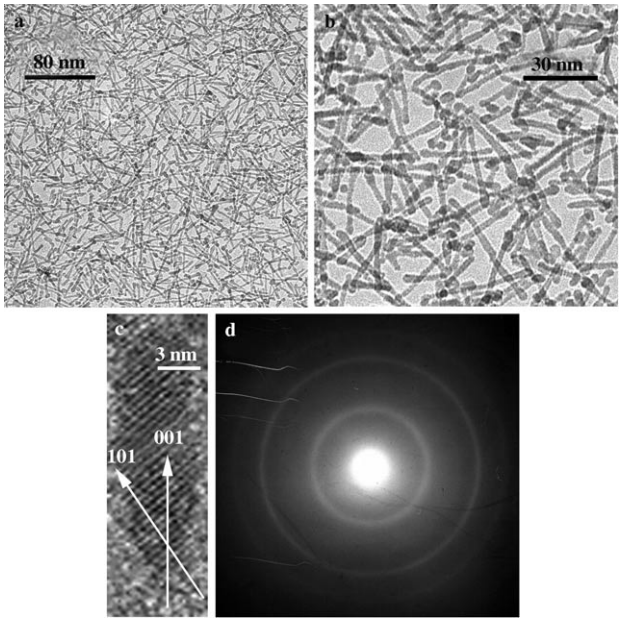

Figure 3. TEM images of TiO_2 nanorods: a,b) images at different magnification, c) HRTEM image of a single nanorod (the lattice fringes are about 0.35 nm), and d) SAED pattern of TiO_2 nanorods.

rods. According to this TEM image, the proportion of rodlike TiO_2 is more than 95%. Figure 3b illustrates a high-magnification TEM image showing that as-synthesized nanorods have an almost uniform diameter of about 3.3 nm (excluding the spherical tip) and length of up to 25 nm. Figure 3c provides a HRTEM image of a single nanorod growing along the (001) direction. The lattice fringes are about

0.35 nm, which can be indexed to the (101) planes of anatase TiO_2. Figure 3d displays the SAED pattern of the nanorods. It indicates that the nanorods are highly crystalline, consistent with the HRTEM images.

Influences of the reaction factors: In our synthesis, a series of experiments have been conducted to get a better understanding of the formation of TiO_2 nanocrystalline particles.

Influences of the amount of LA and NH_4HCO_3: When the temperature is raised to over 150 °C, NH_4HCO_3 will quickly and spontaneously decompose to produce H_2O. LA is an important solvent, crystallizing promoter, coordination surfactant, and hydrolyzation reactant.[23] Thus, in our synthesis, the amount of LA and NH_4HCO_3 are two important factors that will influence the formation of TiO_2. We have carried out a series of control experiments and found that the amount of NH_4HCO_3 and LA have an extremely important influence on the morphology and dispersibility of TiO_2. We have summarized the results of the morphology of TiO_2 obtained at different reaction conditions in Table 1. According to these results, the product morphology changed with the amount of NH_4HCO_3 and LA used.

Table 1. Morphologies of TiO_2 samples obtained under different conditions. In all the reactions $Ti(OBu)_4$ was about 1 mL (3 mmol).

NH_4HCO_3 [g]	LA [mL]	Morphology of TiO_2
0	7	nanorods
0	15	nanorods
0	25	nanorods
0.3	7	elongated nanoparticles
0.3	15	elongated nanoparticles
0.5	0	aggregated particles
0.5	7	nanoparticles
0.5	15	nanoparticles
1	7	nanoparticles
1	25	nanoparticles
4	25	aggregated particles

TiO_2 nanorods were obtained without NH_4HCO_3. When no NH_4HCO_3 was used, the product morphology was determined by the amount of LA. Figure 4 shows TEM images of TiO_2 obtained with different amounts of LA. As shown in Figure 4a–d, the TiO_2 morphology, crystallinity, and dispersibility changed with the amount of LA. When no LA was used, amorphous floccus like structures were obtained (Figure 4a). When the amount of LA was small (about 6 mmol), aggregated particles were obtained (Figure 4b). When the amount of LA was about 21 mmol, crystalline redispersible nanorods of about 25 nm in length were formed (Figure 4c). By increasing the amount of LA further (about 75 mmol), long nanorods (ca. 50 nm) were produced (Figure 4d).

TiO_2 nanoparticles were formed when LA was used in large amounts (75 mmol, 25 mL), and an appropriate amount of NH_4HCO_3 (about 6–25 mmol) was introduced into the reaction system. When NH_4HCO_3 was used, the TiO_2 morphology was mainly determined by NH_4HCO_3: the

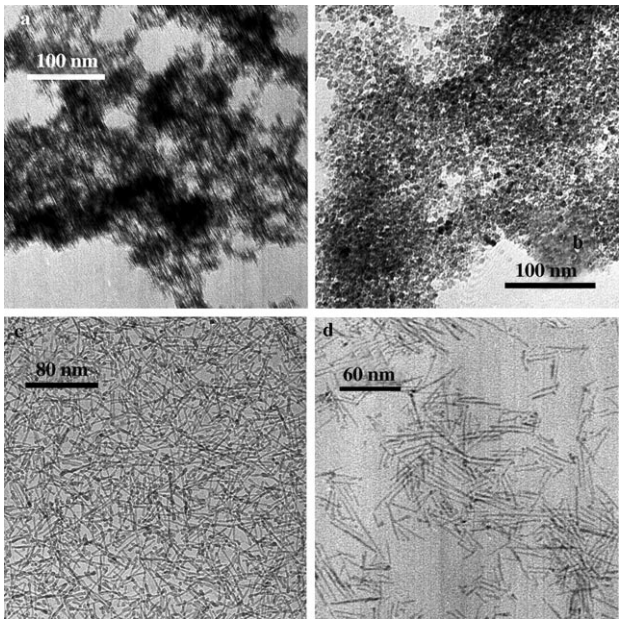

Figure 4. TEM images of TiO_2 obtained with different amounts of LA: a) 0, b) 2, c) 7, and d) 25 mL.

product's morphology did not seem to evolve when the amount of LA was altered, while keeping the amount of NH_4HCO_3 unchanged (see Table 1). However, by changing the amount of NH_4HCO_3 only, the TiO_2 morphology changed from spherical to elongated and aggregated nanoparticles. When the NH_4HCO_3 amount was quite small ($< \approx 6$ mmol), we obtained elongated nanoparticles. When the amount of NH_4HCO_3 was between about 6 and 25 mmol, we obtained nearly spherical nanoparticles. When the amount of NH_4HCO_3 was too large ($> \approx 25$ mmol), we obtained aggregated particles. Figure 5 provides typical

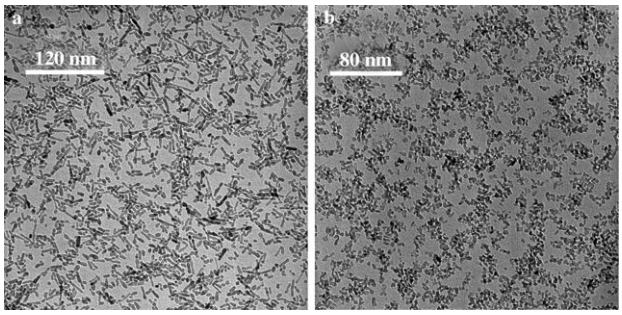

Figure 5. TEM images of TiO_2 obtained with different amounts of NH_4HCO_3 and LA: a) NH_4HCO_3 (0.3 g), LA (7 mL) and b) NH_4HCO_3 (1 g), LA (25 mL).

TEM images of TiO_2 obtained with different amounts of NH_4HCO_3 and LA. Figure 5a shows that elongated TiO_2 particles were obtained with a NH_4HCO_3 concentration of about 4 mmol and a LA concentration of about 21 mmol. Figure 5b shows the near-spherical TiO_2 particles obtained when the amount of NH_4HCO_3 was about 12.5 mmol and that of LA was about 75 mmol.

Based on the experimental evidence above, we believe that the decomposition of NH_4HCO_3 provides H_2O for the hydrolyzation reaction, and LA acts as the solvent and coordination surfactant in the synthesis of nanoparticles. Whereas in the synthesis of nanorods, LA serves as both the hydrolysis reagent to react with $Ti(OBu)_4$ and as a suitable coordination surfactant to promote the anisotropic crystal growth of TiO_2 (polycondensation to form a Ti-O-Ti network). Here, the coordination effect of LA is supported by the re-dispersibility of as-synthesized TiO_2. With LA capping the surface of the growing titania, as-synthesized samples were redispersible in apolar solvents and did not aggregate. If we washed the product excessively with cyclohexane to remove surface-absorbed LA, the TiO_2 nanocrystalline particles were no longer dispersible. By adding some LA they were dispersible in organic solvent again. (Please refer to the Supporting Information for further details of the re-dispersibility of TiO_2.) One unique feature of this reversible binding of LA to the titania surface is that it offers the possibility of post-synthesis attachment of other functional molecules. It has also been found that LA improves the product's crystallinity.

We have also designed control experiments by using different amounts of triethylamine. The results show that triethylamine acts as a catalyst for the polycondensation of the Ti-O-Ti inorganic network to achieve a crystalline product and has little influence on the product's morphology. This is consistent with results from literature.[23]

Influence of the reaction temperature: The reaction temperature has a large influence on the TiO_2 formation. We have investigated the influence of the reaction temperature in the range 100–180 °C and found that highly crystalline TiO_2 nanoparticles and nanorods could only be obtained at temperatures higher than 120 °C, although $Ti(OBu)_4$ can react with LA to form $Ti(OBu)_{4-x}(C_{17}H_{31}CO_2)_x$ at a rather low temperature.[6,7,23,25,29] We carried out the solvothermal reaction at 100 °C, but no TiO_2 could be deposited by alcohol and neither nanoparticles nor nanorods were observed by TEM. However, when the reaction temperature was higher than 120 °C, highly crystalline, near monodisperse and organic-solvent-dispersible TiO_2 nanoparticles were obtained. Figure 6 illustrates the TEM results of TiO_2 nanoparticles obtained at 150 and 180 °C. As shown in the images, these particles are near spherical with similar size of around 10 nm. Figure 7 shows the TEM images of TiO_2 nanorods obtained at 120, 150 and 180 °C. In these images the nanorods have a diameter of 4 nm and length of about 25 nm.

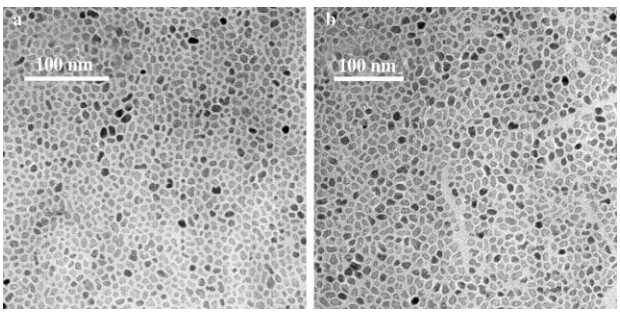

Figure 6. TEM images of TiO_2 nanoparticles obtained at different temperatures: a) 150 and b) 180 °C.

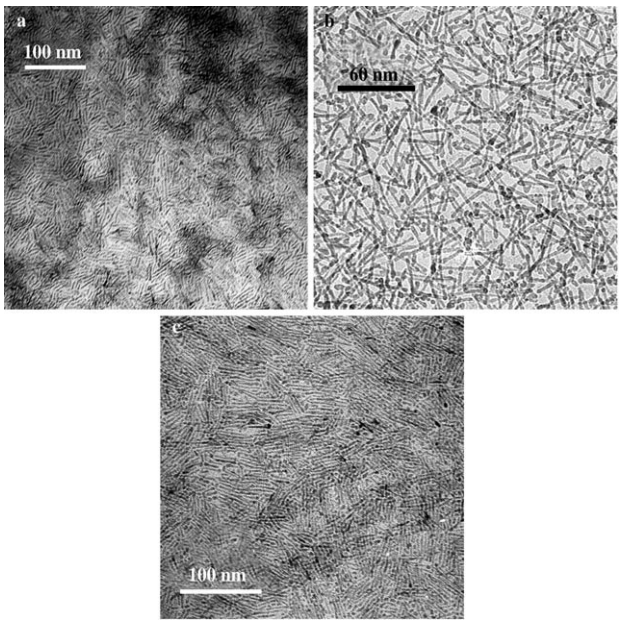

Figure 7. TEM images of TiO_2 nanorods obtained at different temperatures: a) 120, b) 150, and c) 180 °C.

An interesting phenomenon is that nanorods obtained at 150 °C have more spherical particles on the tips. From their HRTEM images (images not shown here) we found that the crystallinity of the products increased with an increase of the reaction temperature, while the size of the products remained mostly unchanged.

Influence of the reaction duration: To investigate the growth processes of TiO_2 nanoparticles and nanorods, we collected samples at different reaction times. The samples were examined by TEM and the typical results are provided in Figures 8 and 9. Figures 8a–e show the TEM images of TiO_2 nanoparticles obtained after 1, 3, 6, 12, and 48 h reaction time, respectively. Figures 9a–e show the TEM images of TiO_2 nanorods obtained after 2, 6, 12, 24, and 48 h reaction time, respectively. From these images, we can see the formation process of TiO_2 nanoparticles and nanorods clearly: crystalline nanoparticles formed after 6 h reaction while crystalline nanorods formed after 12 h reaction. Further observation indicated that with an increase in the reaction duration, the product's crystallinity, size, and dispersibility improved.

Influence of the solvothermal treatment and carboxylic acid types: Solvothermal treatment is very important for the formation of TiO_2 nanocrystalline materials at low tempera-

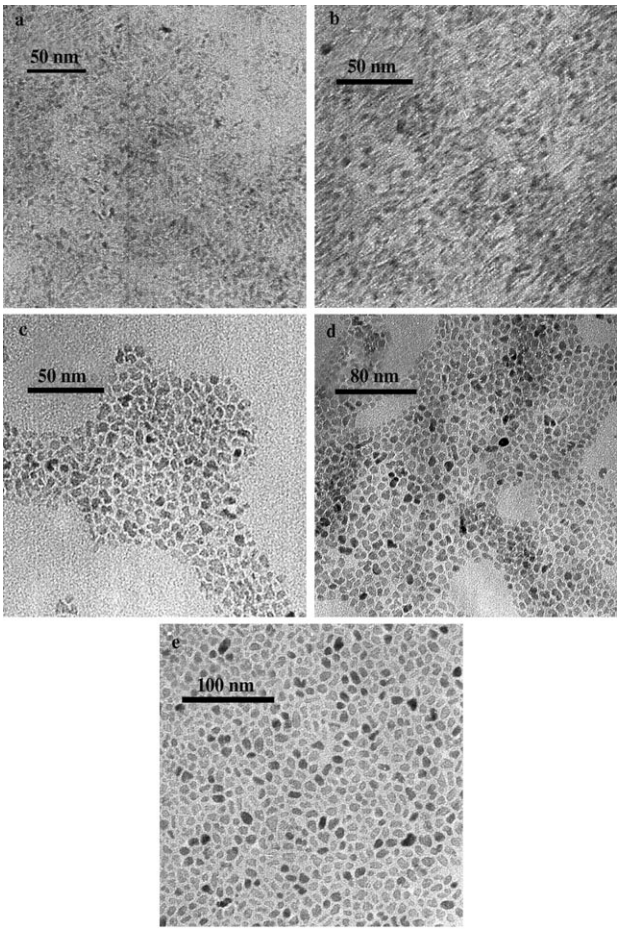

Figure 8. TEM image of TiO_2 nanoparticles obtained at different reaction durations: a) 1, b) 3, c) 6, d) 12, and e) 48 h.

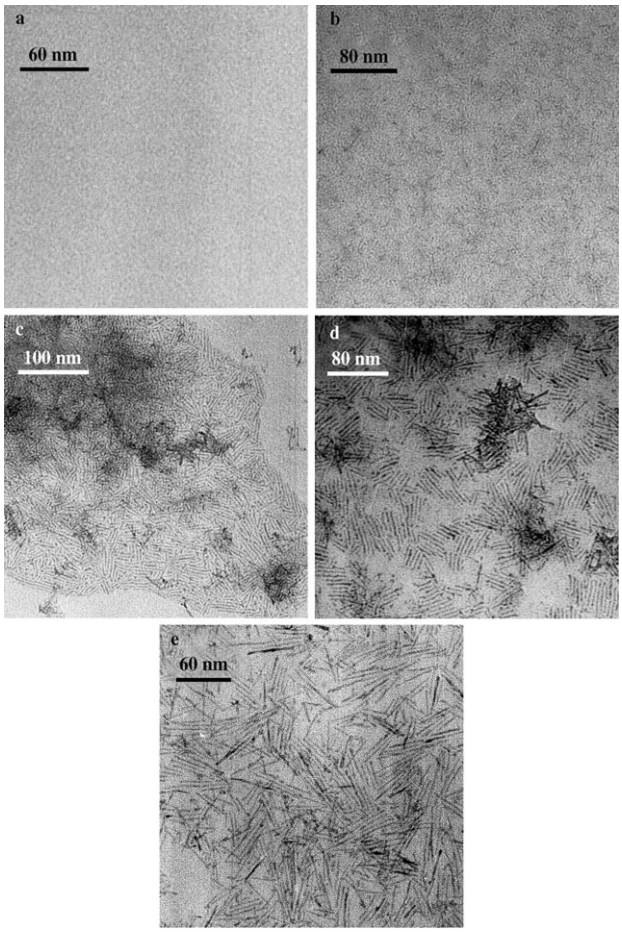

Figure 9. TEM images of TiO_2 nanorods obtained at different reaction durations: a) 2, b) 6, c) 12, d) 24, and e) 48 h.

ture. Highly crystalline nanoparticles were usually obtained at high temperatures.[30–31] For example, CdSe nanocrystalline materials were obtained by heating at 300 °C in trioctylphosphine oxide (TOPO).[30] However, in our reaction system, because the solvent cyclohexane has a very low boiling point (about 80 °C), the reflux temperature is not high enough to achieve crystalline products with conventional solution reflux conditions. As a control, we carried out experiments using a conventional open solution reflux system, but obtained neither nanorods nor nanoparticles. Thus we chose the solvothermal method to obtain highly crystalline TiO_2 at low temperatures. The solvothermal reactions were carried out in a sealed autoclave. It can be considered to be an isochoric closed system, which can provide suitable conditions for the hydrolysis, polycondensation reactions, and the final formation of nanorods and nanoparticles.[32] 1) In the solvothermal system (the volume of the system does not change), the reaction temperature can be heated to 150 °C or more, much higher than the boiling point of cyclohexane. Thus, the reactivity of the reactants might be improved and crystalline TiO_2 could be obtained. 2) The solvothermal system affected the phase transition and nucleation of TiO_2. In this work we obtained pure anatase structured TiO_2. We have recently demonstrated that pure rutile or anatase TiO_2 could be obtained separately in solvothermal systems by using different organic systems. 3) The sealed system prevented the volatilization of the gases (H_2O, CO_2, and NH_3) formed by the decomposition of NH_4HCO_3. Thus H_2O can be kept inside the system to react with $Ti(OBu)_4$ to form the nanoparticles.

The chain length of carboxylic acids also has great influence on the formation TiO_2. We have carried out control experiments using different kinds of carboxylic acids like decanic acid ($C_9H_{19}CO_2H$), valeric acid ($C_4H_9CO_2H$), acetic acid (CH_3CO_2H), and so forth. TiO_2 nanoparticles and nanorods were obtained by using decanic acid; however with valeric acid and acetic acid, TiO_2 deposition did not occur, although the gas chromatography–mass spectrometry (GC-MS) spectra showed that $C_4H_9CO_2Bu$ and CH_3CO_2Bu were formed. Based on these experimental facts, it is believed that long-chain organic acids are important and necessary in the formation of TiO_2.

Reaction mechanism: Formerly reported strategies of the synthesis of TiO_2, especially the hydrolysis reactions of titanium alkoxide reported by Colvin, Alivisatos, Weller, and Niederberger helps in the understanding of the reaction mechanism of TiO_2 nanorods and nanoparticles.[4–7,23–25,29]

Grounded on present available experimental evidence, we assume that this general mechanism of hydrolysis and polycondensation reactions of metal alkoxide might be extended to our system. The nucleation and growth of TiO_2 is known to proceed through two main steps: $Ti(OBu)_4$ first hydrolyses to produce unstable hydroxyalkoxides, then undergoes polycondensation reactions by means of olation or oxolation leading to extensive Ti-O-Ti networks. It is believed that different product structures might be ascribed to the different reaction processes.

TiO_2 nanorods were obtained without NH_4HCO_3. According to the experimental data, LA (about 21 mmol, 7 mL) was believed to serve as both a hydrolysis reagent to react with $Ti(OBu)_4$ and as a suitable coordination surfactant to promote the anisotropic crystal growth of TiO_2 (polycondensation of Ti-O-Ti network). The reaction processes for the formation of TiO_2 nanorods are believed to be as follows.

Titanium alkoxides are known to readily react with carboxylic acids under mild conditions.[4–7,23,29] Mixed alkoxy carboxylates are also formed in the reaction of $Zr(OiPr)_4{\cdot}iPrOH$ with fatty acids .[6] Analogous to the literature, it is believed that titanium alkoxides could also form mixed alkoxy carboxylates with LA [Eq. (1)].

$$Ti(OBu)_4 + x\,C_{17}H_{31}CO_2H \rightarrow Ti(OBu)_{4-x}(C_{17}H_{31}CO_2)_x + x\,BuOH \quad (1)$$

It is well documented in the literature that an oxo bridge could be formed by a condensation reaction between two functional groups bonded to two metal centers and eliminating an organic ester molecule [Eq. (2)]:[4–7,23,25,29]

(2)

Thus, in our system, the nonhydrolytic condensation reaction between the precursors might be able to generate the Ti-O-Ti networks and an eliminated ester. The reactions may include those given in Equation (3) and (4).

$$Ti(OBu)_4 + Ti(OBu)_{4-x}(C_{17}H_{31}CO_2)_x \rightarrow (BuO)_3Ti\text{-}O\text{-}Ti(BuO)_{4-x}(C_{17}H_{31}CO_2)_{x-1} + C_{17}H_{31}CO_2Bu \quad (3)$$

$$n\,Ti(OBu)_{4-x}(C_{17}H_{31}CO_2)_x \rightarrow n/2O\,[\text{-}Ti(BuO)_{3-x}(C_{17}H_{31}CO_2)_{x-1}]_2 + C_{17}H_{31}CO_2Bu \quad (4)$$

The formation of TiO_2 nanorods is a slow process. As shown in Figure 9, we have taken samples at different reaction times and found that no precipitation could be observed when the reaction time was shorter than 12 h. Together with these mild and slow reactions, the effective LA adsorption controls the growth of TiO_2 nuclei into anisotropic, redispersible nanorods.

Based on the experimental results, we believe that the formation of TiO_2 nanoparticles could be ascribed to fast hydrolysis reactions. The reactions are listed below.

By the in situ decomposition of NH_4HCO_3 at high temperature a large amount of H_2O is produced immediately [Eq. (5)].

$$NH_4HCO_3 \rightarrow NH_3 + H_2O + CO_2 \quad (5)$$

With the existence of a large amount of H_2O, the precursors mainly hydrolyze with the water in situ and lead to an immediate, large-scale nucleation and fast crystal growth. The reactions may be as follows [Eq. (6) and (7)]:

$$Ti(OBu)_4 + 2\,H_2O \rightarrow TiO_2 + 4\,BuOH \quad (6)$$

$$Ti(OBu)_{4-x}(C_{17}H_{31}CO_2)_x + 2\,H_2O \rightarrow TiO_2 + (4-x)BuOH + x\,C_{17}H_{31}CO_2H \quad (7)$$

Then, due to the fast crystal growth and LA adsorption, redispersible nanoparticles are obtained. Since the concentration of LA is excessive, the nanoparticles react with BuOH to form esters in both systems [Eq. (8)].

$$BuOH + C_{17}H_{31}CO_2H \rightarrow C_{17}H_{31}CO_2Bu + H_2O \quad (8)$$

The GC-MS results of the reaction products provide strong support for the mechanism. We carried out GC-MS characterization with a synthesis procedure using a small amount of LA to facilitate the identification of the formed organic compounds. The GC-MS results show that the organic product of the hydrolyzation reaction is $C_{17}H_{31}CO_2Bu$, consistent with the reaction mechanism. The inset in Figure 10 shows the GC spectrum, in which the peaks at 2.10, 2.23, and 24.03 are assigned to cyclohexane, triethylamine, and $C_{17}H_{31}CO_2Bu$, respectively. Figure 10 displays the MS spectrum of the peak at 24.03. It matches well with $C_{17}H_{31}CO_2Bu$. We carried out the GC-MS measurement on various samples including the samples obtained at different temperatures and durations. All the spectra exhibited almost the same results.

Metal-doped TiO_2 nanoparticles and nanorods: The solvothermal strategy for the synthesis of TiO_2 can be intermediately applied to the synthesis of metal-doped TiO_2 or other highly crystalline, near monodisperse nanocrystalline materials. Adding a small amount of metal chloride or nitrate into the reaction system, we could obtain metal-doped TiO_2 nanocrystalline materials. Figure 11 provides the typical TEM images and EDX results of Sn^{4+}- (about 0.68 % in weight), Co^{2+}- (about 0.5 % in weight), Fe^{3+}- (about 0.69 % in weight), and Ni^{2+}- (about 0.49 % in weight) doped TiO_2 obtained at 150 °C. The as-synthesized, metal-doped TiO_2 derivatives also have very high crystallinity, near monodisperse size, and good dispersibility in organic solvents. Since

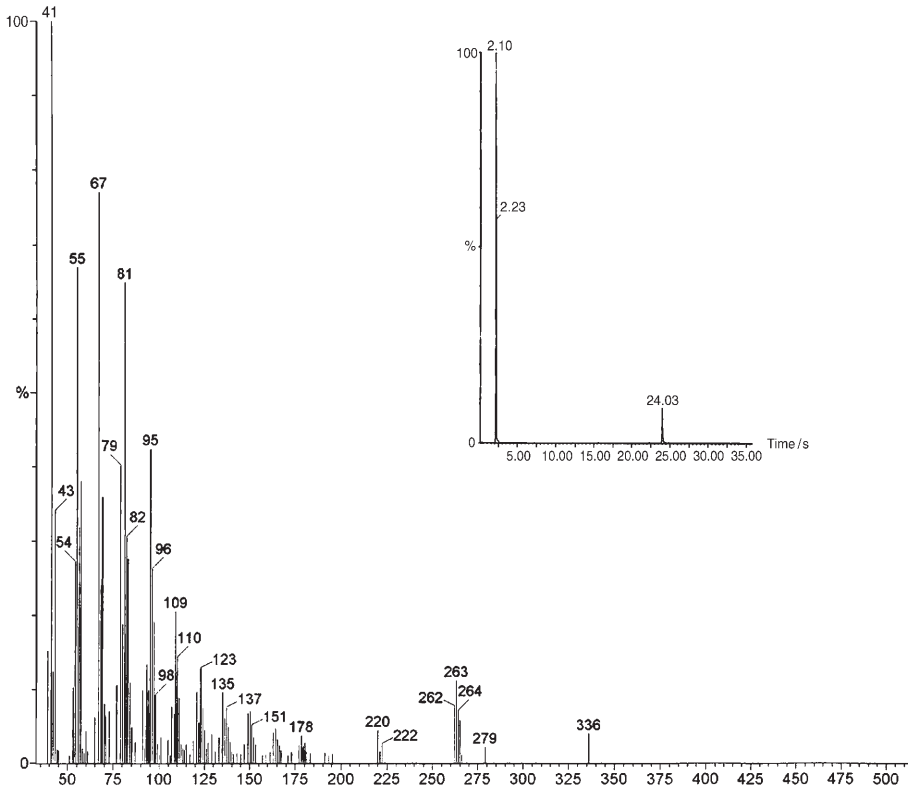

Figure 10. Typical GC-MS results of the hydrolyzation reaction product: the inset shows the GC spectrum and the main figure shows the MS spectrum of the peak at 24.03

the room-temperature ferromagnetism of Co^{2+}-doped TiO_2 was reported, diluted magnetic semiconductors (DMS) of TiO_2 are attracting more and more attention because of their potential applications in spintronics.[33] Controlling the reaction conditions, this strategy might be developed to be an effective method for the synthesis of room-temperature DMS of TiO_2. Synthesis of other metal oxides is still under investigation. This strategy can be expanded to provide a general method for the preparation of highly crystalline, near monodisperse, and redispersible metal oxides.

Conclusion

In summary, we have synthesized highly crystalline, near monodisperse and redispersible TiO_2 nanocrystalline materials, and their metal-ion-doped (such as Sn^{4+}, Fe^{3+}, Co^{2+}, and Ni^{2+}, etc) derivatives by solvothermal reactions. We have fully demonstrated the control of size, shape, dispersibility, and component of TiO_2 through fine adjustment of the reaction parameters. On the basis of the experimental results, we have proposed a possible reaction mechanism to illustrate the formation of TiO_2 nanoparticles and nanorods.

Experimental Section

In the typical synthesis procedure of TiO_2 nanoparticles, NH_4HCO_3 (0.5–2 g), LA (25 mL), triethylamine (5 mL), and cyclohexane (5 mL) were mixed at room temperature by magnetic stirring. Then $Ti(OBu)_4$ (1 mL) was added dropwise into the solution. After continued stirring at room temperature for 5 min, the solution was transferred into a Teflon-lined, stainless autoclave at 150 °C for 24 h.

TiO_2 nanorods were synthesized under well-controlled conditions with an appropriate amount of LA (7 mL) and no NH_4HCO_3. Then $Ti(OBu)_4$ (1 mL) was slowly added dropwise into the mixed solution of LA (7 mL), triethylamine (5 mL), and cyclohexane (20 mL). After the solution was sealed in a Teflon-lined, stainless autoclave at 150 °C for 2 d, TiO_2 nanorods were obtained.

Metal-doped TiO_2 nanoparticles and nanorods were prepared by adding about 2% chlorides into the mixed solution of NH_4HCO_3 (0.5–2 g), LA (25 mL), triethylamine (5 mL), cyclohexane (5 mL), and $Ti(OBu)_4$ (1 mL). After stirring at room temperature for 5 min, the solution was transferred into a Teflon-lined, stainless autoclave at 150 °C for 24 h.

An as-obtained sol of TiO_2 nanocrystalline materials and their doped derivates could be stable for a few weeks. By adding an excess of ethanol to the reaction mixture, TiO_2 nanocrystalline materials were precipitated at room temperature. Before characterization, the resulting precipitates were isolated by centrifugation and washed several times with ethanol to remove surfactant residuals; the residual solvent was evaporated at room temperature. It should be noted that LA-coated TiO_2 nanoparticles were then easily redispersed in solvents such as chloroform or cyclohexane, without any further growth or irreversible aggregation. If washing of the precipitate was repeated too many times, the products generally resulted by precipitation in apolar solvents. Upon the addition of a small amount of fresh LA (a few drops), complete dispersibility could be recovered.

Acknowledgements

This work was supported by NSFC (50372030, 20131030), the Specialized Research Fund for the Doctoral Program of Higher Education, the Foundation for the Author of National Excellent Doctoral Dissertation of P. R. China and the state key project of fundamental research for nanomaterials and nanostructures (2003CB716901).

[1] B. L. Cushing, V. L. Kolesnichenko, C. J. O'Connor, *Chem. Rev.* **2004**, *104*, 3893–3946.
[2] C. D. Chandler, C. Roger, M. J. Hampdensmith, *Chem. Rev.* **1993**, *93*, 1205–1241.
[3] a) R. C. Mehrotra, A. Singh. *Inorg. Chem.* **1997**, *46*, 239–454; b) R. Bohra, *J. Indian Chem. Soc.* **2005**, *82*, 197–213.
[4] A. Vioux, *Chem. Mater.* **1997**, *9*, 2292–2299.

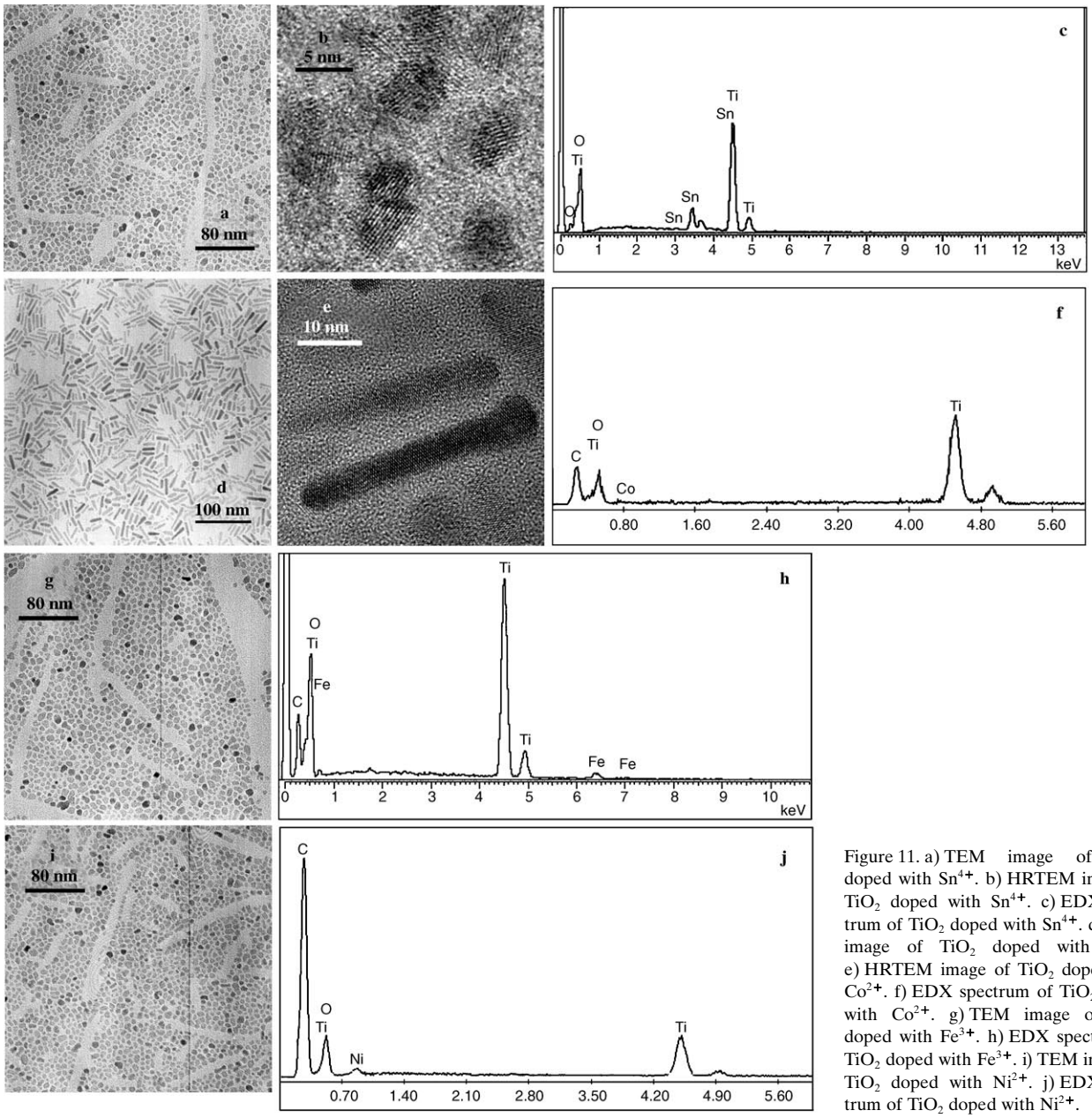

Figure 11. a) TEM image of TiO_2 doped with Sn^{4+}. b) HRTEM image of TiO_2 doped with Sn^{4+}. c) EDX spectrum of TiO_2 doped with Sn^{4+}. d) TEM image of TiO_2 doped with Co^{2+}. e) HRTEM image of TiO_2 doped with Co^{2+}. f) EDX spectrum of TiO_2 doped with Co^{2+}. g) TEM image of TiO_2 doped with Fe^{3+}. h) EDX spectrum of TiO_2 doped with Fe^{3+}. i) TEM image of TiO_2 doped with Ni^{2+}. j) EDX spectrum of TiO_2 doped with Ni^{2+}.

[5] a) J. N. Hay, H. M. Raval, *Chem. Mater.* **2001**, *13*, 3396–3403; b) U. Schubert, N. Husing, A. Lorenz, *Chem. Mater.* **1995**, *7*, 2010–2027.
[6] a) U. Schubert, E. Arpac, W. Glaubitt, A. Helmerich, C. Chau, *Chem. Mater.* **1992**, *4*, 291–295; U. Schubert, S. Tewinkel, R. Lamber, *Chem. Mater.* **1996**, *8*, 2047–2055.
[7] T. J. Boyle, R. P. Tyner, T. M. Alam, B. L. Scott, J. W. Ziller, B. G. Potter Jr. , *J. Am. Chem. Soc.* **1999**, *121*, 12104–12112.
[8] a) B. O'Regan, M. Gratzel, *Nature* **1991**, *353*, 737–739; b) M. Gratzel, *Nature* **2001**, *414*, 338–344; c) M. Wagemaker, A. P. M. Kentgens, F. M. Mulder, *Nature* **2002**, *418*, 397–399; d) P. Wang, S. M. Zakeeruddin, J. E. Moser, M. K. Nazeeruddin, T. Sekiguchi, M. Gratzel, *Nat. Mater.* **2003**, *2*, 402–407.
[9] a) R. Asahi, T. Morikawa, T. Ohwaki, K. Aoki, Y. Taga, *Science* **2001**, *293*, 269–271; b) P. G. Smirniotis, D. A. Pena, B. S. Uphade, *Angew. Chem.* **2001**, *113*, 2537–2540; *Angew. Chem. Int. Ed.* **2001**, *40*, 2479–2482.
[10] a) A. Fujishima, K. Honda, *Nature* **1972**, *238*, 37; b) S. U. M. Khan, M. Al-Shahry, W. B. Ingler, *Science* **2002**, *297*, 2243–2245.
[11] a) W. Zhao, W. H. Ma, C. H. Chen, J. C. Zhao, Z. G. Shuai, *J. Am. Chem. Soc.* **2004**, *126*, 4782–4783; b) W. Zhao, C. C. Chen, X. Z. Li, J. C. Zhao, H. Hidaka, N. Serpone, *J. Phys. Chem. B* **2002**, *106*, 5022–5028.
[12] R. Wang, K. Hashimoto, A. Fujishima, M. Chikuni, E. Kojima, A. Kitamura, M. Shimohigoshi, T. Watanabe, *Nature* **1997**, *388*, 431–432.
[13] C. Bechinger, S. Ferrere, A. Zaban, J. Sprague, B. A. Gregg, *Nature* **1996**, *383*, 608–610.
[14] T. Paunesku, T. Rajh, G. Wiederrecht, J. Maser, S. Vogt, N. Stojicevic, M. Protic, B. Lai, J. Oryhon, M. Thurnauer, G. Woloschak, *Nat. Mater.* **2003**, *2*, 343–346.
[15] a) J. E. G. J. Wijnhoven, W. L. Vos, *Science* **1998**, *281*, 802–804; b) M. C. Carotta, M. Ferroni, V. Guidi, G. Martinelli, *Adv. Mater.*

1999, *11*, 943–946; c) Y. Matsumoto, M. Murakami, T. Shono, T. Hasegawa, T. Fukumura, M. Kawasaki, P. Ahmet, T. Chikyow, S. Koshihara, H. Koinuma, *Science* **2001**, *291*, 854–856; d) Y. Ohko, T. Tatsuma, T. Fujii, K. Naoi, C. Niwa, Y. Kubota, A. Fujishima, *Nat. Mater.* **2003**, *2*, 29–31.
[16] D. L. Li, H. S. Zhou, I. Honma, *Nat. Mater.* **2004**, *3*, 65–72.
[17] K. Kanie, T. Sugimoto, *J. Am. Chem. Soc.* **2003**, *125*, 10518–10519.
[18] X. C. Jiang, T. Herricks, Y. N. Xia, *Adv. Mater.* **2003**, *15*, 1205–1209.
[19] a) E. Hosono, S. Fujihara, K. Kakiuchi, H. Imai, *J. Am. Chem. Soc.* **2004**, *126*, 7790–7791; b) Z. R. R. Tian, J. A. Voigt, J. Liu, B. Mckenzie, H. F. Xu, *J. Am. Chem. Soc.* **2003**, *125*, 12384–12385.
[20] Y. Zhou, M. Antonietti, *J. Am. Chem. Soc.* **2003**, *125*, 14960–14961.
[21] S. J. Limmer, G. Z. Cao, *Adv. Mater.* **2003**, *15*, 427–431.
[22] T. J. Trentler, T. E. Denler, J. F. Bertone, A. Agrawal, V. L. Colvin, *J. Am. Chem. Soc.* **1999**, *121*, 1613–1614.
[23] a) P. D. Cozzoli, A. Kornowski, H. Weller, *J. Am. Chem. Soc.* **2003**, *125*, 14539–14548; b) Y. W. Jun, M. F. Casula, J. H. Sim, S. Y. Kim, J. W. Cheon, A. P. Alivisatos, *J. Am. Chem. Soc.* **2003**, *125*, 15981–15985.
[24] a) M. Niederberger, G. Garnweitner, N. Pinna, M. Antonietti, *J. Am. Chem. Soc.* **2004**, *126*, 9120–9126; b) M. Niederberger, M. H. Bartl, G. D. Stucky, *Chem. Mater.* **2002**, *14*, 4364–4370.
[25] a) P. Arnal, R. J. P. Corriu, D. Leclercq, P. H. Mutin, A. Vioux, *Chem. Mater.* **1997**, *9*, 694–698; b) V. Lafond, P. H. Mutin, A. Vioux, *Chem. Mater.* **2004**, *16*, 5380–5386; c) L. Crouzet, D Leclereq, P. H. Mutin, A. Vioux, *Chem. Mater.* **2003**, *15*, 1530–1534.
[26] a) C. Wang, Z. X. Deng, Y. D. Li, *Inorg. Chem.* **2001**, *40*, 5210–5214; b) C. Wang, Z. X. Deng, G. H. Zhang, S. S. Fan, Y. D. Li, *Powder Technol.* **2002**, *125*, 39–44.
[27] X. L. Li, J. F. Liu, X. Wang, Q. Peng, Y. P. Zhang, Y. D. Li, unpublished results.
[28] X. Wang, Y. D. Li, *Nature*, **2005**, *437*, 121–124.
[29] S. Doeuff, Y. Dromzee, F. Taulelle, C. Sanchez, *Inorg. Chem.* **1989**, *28*, 4439–4445.
[30] a) A. P. Alivisatos, *Science* **1996**, *271*, 933–937; b) X. G. Peng, L. Manna, W. D. Yang, J. Wickham, E. Scher, A Kadavanich, A. P. Alivisatos, *Nature* **2000**, *404*, 59–61.
[31] a) X. G. Peng, *Adv. Mater.* **2003**, *15*, 459–463; b) Z. A. Peng, X. G. Peng, *J. Am. Chem. Soc.* **2001**, *123*, 1389–1395.
[32] a) R. I. Walton, *Chem. Soc. Rev.* **2002**, *31*, 230–238; b) S. H. Yu, *J. Ceram. Soc. Jpn.* **2001**, *109*, 65–75.
[33] a) S. A. Chambers, S. Thevuthasan, R. F. C. Farrow, R. F. Marks, J. U. Thiele, L. Folks, M. G. Samant, A. J. Kellock, N. Ruzycki, D. L. Ederer, U. Diebold, *Appl. Phys. Lett.* **2001**, *79*, 3467–3469; b) J. D. Bryan, S. M. Heald, S. A. Chambers, D. R. Gamelin, *J. Am. Chem. Soc.* **2004**, *126*, 11640.

Received: July 27, 2005
Published online: December 23, 2005

